Magnetism and Optical Transparency in Ru-doped $BaSnO_3$ Epitaxial Thin Films

Emily R. Lindgren[1,2] and Yuri Suzuki[1,3]
[1)] *Geballe Laboratory for Advanced Materials, Stanford University*
[2)] *Department of Materials Science and Engineering, Stanford University*
[3)] *Department of Applied Physics, Stanford University*

(Dated: March 31, 2023)

We have stabilized epitaxial oxide thin films of transparent, magnetic Ru-doped $BaSnO_3$. Films were grown by pulsed laser deposition and exhibited excellent epitaxy and crystallinity as determined by x-ray diffraction. Epitaxial films of Ru doped $BaSnO_3$ were grown with a ceramic target of nominally 4% Ru doping on the Sn site but resulted in 3% Ru doping in the films. Paramagnetic behavior is observed in all films with a Curie law dependence on temperature. The field dependence of the magnetization shows a paramagnetic moment that saturates at a value consistent with low spin Ru. Films are also found to be transparent in the visible regime. Together these results demonstrate the realization of highly crystalline, transparent, paramagnetic, eptiaxial doped $BaSnO_3$ films.

I. INTRODUCTION

Complex oxides exhibit a wide range of electronic, magnetic and optical properties and have been identified as promising materials for an oxide-based electronics. Among the complex oxides, doped barium stannates are semiconductors that have sufficiently high mobility to be integrated into and form the basis of an all-oxide electronics. In addition to high mobility they also exhibit optical transparency in the visible wavelength regime, making them candidates for applications in transparent electronics and opto-electronic devices. For example, $BaSnO_3$ has a wide band gap of 3.4 eV and can be n-type doped on the Ba site to have high room temperature mobilities, up to 180 cm^2/Vs in thin films.[1] Additional magnetic functionality in such a high mobility semiconductor would make doped stannates more versatile. In fact there has been considerable research on ferromagnetic semiconductors, such as GaMnAs, where magnetic dopants have been incorporated into a semiconductor parent compound.[2]The discovery of new ferromagnetic semiconductors has the potential to enable a new type of microelectronics – spintronics – that exhibits non-volatility, added spin functionality and potential improvement in energy efficiency beyond the traditional charge-based microelectronics. This work explores and characterizes magnetic Ru doping of $BaSnO_3$, and identifies Ru doping as a promising avenue for the realization of spin polarization in the transparent conducting oxide $Ba_{1-x}La_xSnO_3$.

There has already been some success in producing a magnetic response in the stannates exploiting the dilute magnetic semiconductor approach applied to III-V semiconductors as well as oxide semiconductors such as ZnO, TiO_2 and SnO_2.[3–5] One approach to realize magnetic functionality in the $BaSnO_3$ system has been to dope the Ba site with rare earth elements such as Gd, Nd, Pr.[6–8] This has resulted in paramagnetic ordering with moments localized to the donor dopant, but ferromagnetism has not been achieved likely due to the weaker exchange interactions among Ba (or A) site ions.

Other studies have incorporated 3d transition metal ions, such as Fe, Mn, Cr and Co onto the Sn $^{4+}$ site to show evidence of room temperature ferromagnetism.[9–15]The observed ferromagnetism has been explained in terms of F center exchange interactions, in which oxygen vacancy trapping of electrons gives rise to the ferromagnetic ordering, but could also be explained in terms of dopant clustering or contamination. Due to the multivalent nature of these 3d transition metal ions, doping of the Sn site with 3d transition metals inevitably leads to aliovalent doping; such aliovalent doping results in trapping of charge carriers and thus counters any attempt to increase conductivity via La doping on the Ba site. Therefore isovalent doping of the Sn site with magnetic ions is a promising pathway to magnetically dope stannates in combination with rare earth doping of the Ba site to provide high mobility conduction.

A promising approach to generating a ferromagnetic response in $BaSnO_3$ is to incorporate isovalent 4d transition metal Ru^{4+} doping on the Sn^{4+} site since in an octahedral coordination Ru^{4+} has an ionic radius closer to that of Sn^{4+} than the 3d transition metal ions described above. While complete substitution of the Sn with Ru results in a number of hexagonal phases of $BaRuO_3$,[16–18] ferromagnetism has been known to be stabilized in a cubic perovskite structure, under high pressure synthesis.[19–21] However with low Ru doping in the cubic $BaSnO_3$ lattice, magnetic functionality may be generated while maintaining the cubic perovskite crystal structure. There has been one bulk study attempting Ru doping, but these authors have found Ru doping on the Ba site with ferromagnetism attributed to oxygen vacancies and not with Ru doping.[22] While low Ru doping that retains the perovskite structure may not result in long range magnetic order, the effect of Ru doping of the Sn or B site has yet to be explored.

In this paper, we demonstrate the stabilization of epitaxial films of nominally 4%Ru doped $BaSnO_3$ grown on $SrTiO_3$ single crystal substrates. X-ray diffraction

measurements indicate excellent epitaxy and crystallinity as determined from the small mosaic spread of the film peaks. X-ray fluorescence enables us to estimate the Ru doping level in our films to be 3%. Optical transparency of these doped films are comparable to those of the undoped films and the $SrTiO_3$ substrates. Ru-doped $BaSnO_3$ films are insulating at room temperature, as is expected without the addition of rare earth doping on the Ba site. Our 3% Ru doped films exhibit paramagnetic behavior down to 5K. The saturated paramagnetic moment at 5K corresponds to low spin Ru^{4+} ions of 1.6 μ_B. While a ferromagnetic state was not stabilized at 3% Ru doping, the observation of a strong paramagnetic response indicates that increased Ru concentration may be a viable route towards a ferromagnetic ground state that could be incorporated into a transparent conductor through co-doping of isovalent Sn^{4+} with Ru^{4+} and rare earth doping of Ba^{2+}.

II. EXPERIMENTAL METHODS

Barium stannate thin films were grown by pulsed laser deposition (PLD) on (001) oriented $SrTiO_3$ (STO) substrates. A 248nm eximer KrF laser was used with an energy density of approximately 1.67 J/cm^2 and a frequency of 3Hz to ablate the sintered ceramic target with a nominal composition of $BaSn_{0.96}Ru_{0.04}O_3$ (Toshima Manufacturing Company). Films were grown at 750°C in an atmoshpere of 100 mTorr of O_2 and subsequently cooled to room temperature in 600 mTorr of O_2.

Structural characterization was performed on a Panalytical Empyrean x-ray diffractometer with a Cu $K_{\alpha 1}$ source in the triple axis geometry. $2\theta/\omega$ scans and ω-rocking curves were taken to verify epitaxial growth and crystalline quality. X-ray reflectivity (XRR) was performed using a Panalytical X'Pert x-ray diffractometer to deduce film roughness and thickness. Atomic Force Microscopy (AFM) was performed on a Digital Instruments Dimension 3100 AFM to quantify surface roughness. Dopant incorporation was verified initially with X-ray Photoelectron Specroscopy (XPS) on a PHI VersaProbe 3 XPS and composition was estimated with X-ray fluorescence spectroscopy (XRF) on a Rigaku Primus II Wavelength Dispersive XRF Instrument with a Rhodium x-ray source. SQUID Magnetometry was performed in a Quantum Design Evercool Magnetic Property Measurement System (MPMS) using the reciprocating sample option (RSO). The substrate for each sample was measured prior to growth to screen for paramagnetic impurity signals and ensure an accurate background subtraction. Samples were field cooled at 7T and field dependent magnetization measurements were taken in-plane, along the {100} direction at 5K. The temperature dependence of the magnetization was also measured between 5-300K at 1000 Oe. Optical measurements of transmission were performed on an Agilent Cary 6000i UV/Vis/NIR Spectrophotometer.

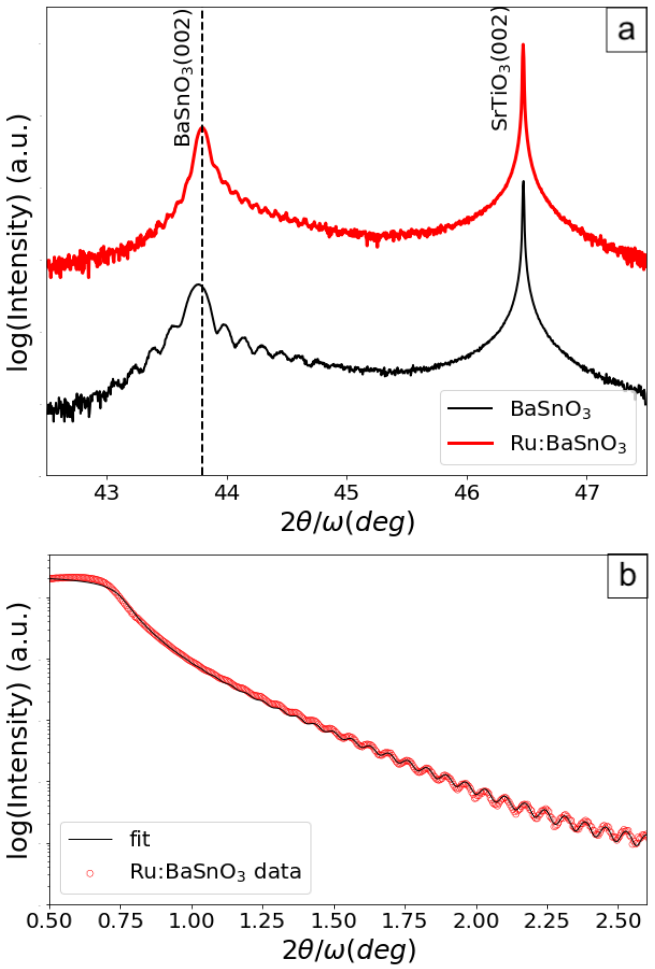

Figure 1. (a) X-ray diffraction spectra of 118 nm thick Ru: $BaSnO_3$ film and 56nm undoped $BaSnO_3$ film; (b) x-ray reflectivity of the 118 nm Ru: $BaSnO_3$ film and corresponding fit.

III. RESULTS & DISCUSSION

A. Structure

Symmetric X-ray diffraction measurements confirm high crystalline quality of $BaSnO_3$ films grown in the (001) orientation on $SrTiO_3$. 2θ-θ measurements were performed between 2θ=15-80° and the only features present in spectra were attributed to the (00l) family of peaks for the $BaSnO_3$ films and $SrTiO_3$ substrates. Laue oscillations are visible in doped and undoped samples around the (002) peak of $BaSnO_3$(Figure 1(a)). The (002) peak is found at approximately 43.8° in Ru: $BaSnO_3$ films and corresponds to a c-axis lattice parameter of 4.1305$\mathring{A}$, closely matching the bulk lattice parameter for $BaSnO_3$ of 4.116 $\mathring{A}$. The slight expansion of the out-of-plane lattice parameter is consistent with the in-plane compressive strain imposed by the smaller $SrTiO_3$ lattice. Omega rocking curve scans of comparable

Ru: $BaSnO_3$ films have a characteristic FWHM ranging between 0.03 - 0.04° indicating high crystalline quality. XRR data of the samples were fit to determine thickness and film roughness. Figure 1(b) shows an XRR scan of the Ru: $BaSnO_3$ sample in Figure 1(a), indicating a film roughness of approximately 1nm and film thickness of 118nm. This roughness is consistent with AFM measurements that indicate typical rms roughness values of 1.1nm for films between 80-120 nm thick.

B. Composition

The nominal target composition is $BaSn_{0.96}Ru_{0.04}O_3$, but due to the volatility of Ru atoms during growth, the resultant Ru concentration in the film is reduced from the amount of Ru in the target. Thus compositional measurements on the resultant films are required to assess dopant transfer into the film. However low Ru dopant concentration is difficult to assess. Due to the low X-ray cross section of Ru, Ru content was verified in the films with XPS, but quantitative Ru concentration values were only obtained using XRF. XRF of our films indicates a 3% Ru concentration. The XRF results were quantified with Fundamental Parameters standard-less quantification software with an error of up to 20% for trace elements, indicating a film composition of $BaSn_{0.97\pm0.002}Ru_{0.03\pm0.002}O_3$. The error in dopant analysis makes quantifying the magnetic response particularly challenging.

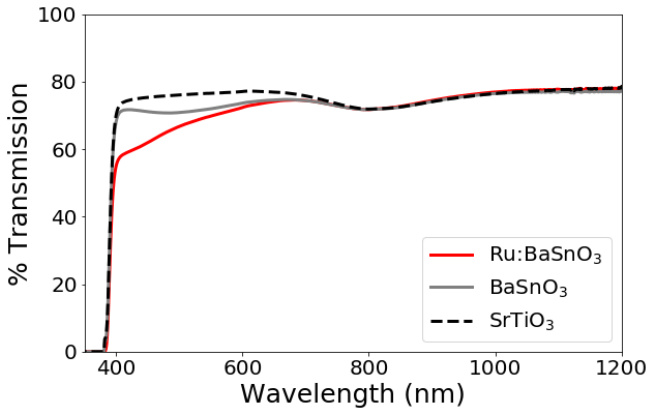

Figure 2. Transmission spectra between 375nm-1200nm of undoped BSO, Ru:BSO and an STO substrate.

C. Optical Properties

The optical transmission of doped and undoped $BaSnO_3$ samples as well as bare $SrTiO_3$ substrates show transparency in the visible and near infrared wavelength regimes. The transmission spectra of doped and undoped $BaSnO_3$ films are shown in Figure 2 between 375-1200nm. The sharp drop off in transmission at 380nm corresponds to the 3.25eV band gap of the $SrTiO_3$ substrate. The measurements are a function of the thickness of the material and the transmissivity of the substrate as well as the intrinsic film properties. The films shown in Figure 2 are both approximately 100nm thick and shows similar transmission behavior above 500nm or so extending into the near infrared. However a number of Ru doped samples show suppression of transmission in the 400-600nm range, suggesting that Ru dopants facilitate absorption in the violet part of the visible spectrum. However doping of the $BaSnO_3$ films, in general, does not affect the optical transparency significantly.

D. Magnetism

Magnetization measurements indicate a diamagnetic response in the undoped $BaSnO_3$ films, and a paramagnetic response corresponding to the Ru^{4+} dopants in the Ru:$BaSnO_3$ films. We observe paramagnetic behavior in these films down to 5K that saturates at approximately 1.6 μ_B/Ru atom. The magnetization data fit well to a Brillouin function describing the magnetic response of an ideal paramagnet. The temperature dependence of the magnetic moment shows a magnetization that is inversely proportional to temperature. This behavior is characteristic of a paramagnet obeying Curie's law. The inset of Figure 2 shows the typical behavior of our doped films that were field cooled in 7T and then measured in a field of 1000 Oe.

The Ru^{4+} ions are thought to substitute for the Sn ions on the octahedrally coordinated B sites of the ABO_3 perovskite structure. This octahedral coordination results in crystal field splitting of the Ru 4d orbitals into the t_{2g} and e_g levels. Due to the magnitude of the crystal field splitting, we expect a low spin state for Ru ions as is the case for most 3d and 4d transition metal ions. A low spin states translates into $2\mu_B$/Ru atom. We measure a lower moment of 1.6 μ_B/Ru atom at 5K. This value is lower than the theoretical maximum but is still higher than the Ru moment deduced in itinerant ferromagnets, such as in $SrRuO_3$.[23] Given the isolated nature of the Ru dopants in our Ru:$BaSnO_3$ films versus the itinerancy of the magnetism in $SrRuO_3$, it is not too surprising that we observe a higher Ru moment in Ru:$BaSnO_3$ compared to $SrRuO_3$.

For stabilization of long range magnetic order, it is clear that significantly more Ru doping is required. When the B site is entirely occupied by Ru ions in the ruthenates (AE)RuO_3 (AE=Ca, Sr, Ba), the magnetic behavior depends on the alkaline earth ion choice.[21,24] $CaRuO_3$ stabilizes in the orthorhombic Pnma crystal structure and behaves like a paramagnet down to very low temperature. When the Ca is replaced with Sr, the crystal structure maintains the orthorhombic Pnma structure but with less RuO_6 octahedral distortions. $SrRuO_3$ exhibits itinerant ferromagnetism with a Curie temperature of about 160K.[23,25] $BaRuO_3$ can be sta-

bilized in the cubic perovskite structure with $Pm\bar{3}m$ space group under high pressure synthesis but also has a number of different hexagonal 9R, 6H, and 4H polymorphs polytypes.[19,21] The perovskite phase of $BaRuO_3$ exhibits ferromagnetism with a Curie temperature of about 60K.[19] Structural distortions of the Ru-O-Ru bonds toward a more cubic structure appear to be important in stabilizing long range magnetic order in the ruthenates.[19,24,26–28] Given the ferromagnetic properties of cubic $BaRuO_3$ (albeit only stable under high pressure synthesis), it may be possible to stabilize a ferromagnetic ground state in $BaSnO_3$ at a higher Ru-doping level.

As expected, Ru-doping of $BaSnO_3$ films did not change the electronic properties from that of insulating undoped $BaSnO_3$ films. In any case, if isovalent Ru doping of the Sn site could provide magnetic functionality, then it could be combined with rare earth doping of the Ba site that has been shown to generate high mobility in $BaSnO_3$.[1,7,15] Our attempts at co-doping of La and Ru ions into $BaSnO_3$ using pulsed laser deposition have been unsuccessful, likely due to the cation disorder stemming from multiple dopants on both cation sites and lower crystalline quality. Although all of our co-doped samples are non-magnetic and insulating, atomically accurate placement of dopants via oxide molecular beam epitaxy techniques may enable the realization of transparency, magnetism and conductivity.

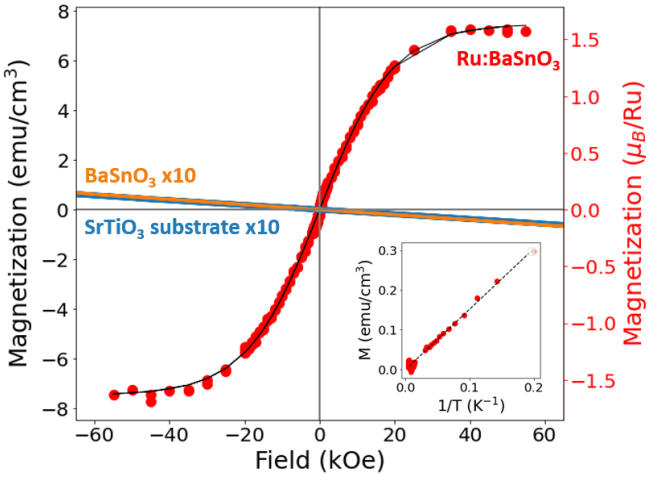

Figure 3. Magnetization of Ru doped $BaSnO_3$ film at 5K after field cooling at 7T after background subtraction. The fit to the Brillouin function is shown in black. The corresponding diamagnetic STO substrate before growth and a characteristic undoped BSO film are shown at 10x amplification. Inset shows temperature dependence of magnetization of Ru: $BaSnO_3$ films at a field of 1000 Oe, and the fit in black to Curie's Law with agreement.

IV. CONCLUSION

In summary, we have demonstrated the synthesis of 3% Ru-doped $BaSnO_3$ epitaxial thin films with good crystalline quality. The films show high optical transparency in the visible and IR range. Bulk magnetometry measurements show that these Ru:$BaSnO_3$ films exhibit a strong paramagnetic response, indicating that 3% Ru doping is not sufficient to achieve ferromagnetic ordering in this system. Understanding the growth conditions and magnetic behavior of Ru-doped $BaSnO_3$ is an important step towards towards the realization of co-doped multi-functional $BaSnO_3$ films.

V. ACKNOWLEDGMENTS

E.R.L. is grateful to Sanyum Channa and Charles Zheng for useful discussions. This work was supported by the National Science Foundation on Award No. 1762971 and 2037652. Part of this work was performed at the Stanford Nano Shared Facilities under NSF Award No. EECS-1542152. XRF measurements were performed by EAG Laboratories. This research used resources of the Advanced Light Source, which is a DOE Office of Science User Facility under contract no. DE-AC02-05CH11231.

REFERENCES

[1] Hanjong Paik, Zhen Chen, Edward Lochocki, Ariel Seidner H., Amit Verma, Nichola Tanen, Park Jisung, Masaki Uchida, ShunLi Shang, BiCheng Zhou, Mario Brutzam, Reinhard Uecker, Zi-Kui Liu, Debdeep Jena, Kyle M. Shen, David A. Muller, and Darrell G Schlom. Adsorption-controlled growth of La-doped BaSnO3 by molecular-beam epitaxy. *APL Materials*, 36:116107–1, 2017.

[2] Tomasz Dietl. A ten-year perspective on dilute magnetic semiconductors and oxides. *Nature Materials*, 9:965–974, 2010.

[3] J. M. D. Coey, A. P. Douvalis, C. B. Fitzgerald, and M. Venkatesan. Ferromagnetism in Fe-doped SnO_2 thin films. *Appl. Phys. Lett.*, 84(8):1332, 2004.

[4] Nguyen Hoa Hong, Joe Sakai, Nathalie Poirot, and Virginie Brize. Room-temperature ferromagnetism observed in undoped semiconducting and insulating oxide thin films. *Phys. Rev. B*, 73, 2006.

[5] H. Chou, C.P. Lin, Huang J.C.A., and H.S. Hsu. Magnetic coupling and electric conduction in oxide diluted magnetic semiconductors. *Phys. Rev. B*, 77, 2008.

[6] Urusa S. Alaan, Padraic Shafer, Alpha T. N'Diaye, Elke Arenholz, and Y. Suzuki. Gd-doped $BaSnO_3$: A transparent conducting oxide with localized magnetic moments. *Appl. Phys. Lett.*, 108:042106, 2016.

[7] Eric McCalla, Daniel Phelan, Matthew J. Krogstad, Bogdan Dabrowski, and Chris Leighton. Electrical transport, magnetic and thermodynamic properties of la, pr and nd doped $basno_{3-\delta}$ single crystals. *Phys. Rev. Mater.*, 2:084601, 2018.

[8] Fang-Yuan Fan, Wei-Yao Zhao, Ting-Wei Chen, Jian-Min Yan, Jin-Peng Ma, Lei Guo, Guan-Yin Gao, Fei-Fei Wang, and Ren-Kui Zheng. Excellent structural, optical, and electrical properties of nd-doped $basno_3$ transparent thin films. *Appl. Phys. Lett.*, 113:202102, 2018.

[9] K. Balamurugan, N. Harish Kumar, J. Arout Chelvane, and P.N. Santhosh. Room temperature ferromagnetism in Fe-doped $BaSnO_3$. *J. Alloys Comp.*, 472(1-2):9–12, 2009.

[10] K. Balamurugan, N. Harish Kumar, B. Ramachandran, M.S. Ramachandra Rao, J. Arout Chelvane, and P.N. Santhosh. Magnetic and optical properties of Mn-doped $BaSnO_3$. *Solid State Comm.*, 149(21-22):884–887, 2009.

[11] Qinzhuang Liu, Yunhua He, Hong Li, Bing Li, Guanyin Gao, Lele Fan, and Jianming Dai. Room-temperature ferromagnetism in transparent Mn-doped $BaSnO_3$ epitaxial films. *Appl. Phys. Exp.*, 7:033006, 2014.

[12] K.K. James, Arun Aravind, and M.K. Jayaraj. Structural, optical and magnetic properties of Fe-doped barium stannate thin films grown by PLD. *Appl. Surface Science*, 282:121–125, 2013.

[13] Urusa S. Alaan, Alpha T. N'Diaye, Padraic Shafer, Elke Arenholz, and Yuri Suzuki. Structure and magnetism of Fe-doped $BaSnO_3$ thin films. *AIP Advances*, 7(5):1–8, 2017.

[14] O Parkash, D Kumar, K K Srivastav, and R K Dwivedi. Electrical conduction behaviour of cobalt substituted $BaSnO_3$. *Journal of Materials Science*, 36:5805–5810, 2001.

[15] Urusa S. Alaan, Franklin J. Wong, Jeffrey J. Ditto, Alexander W. Robertson, Emily Lindgren, Abhinav Prakash, Greg Haugstad, Padraic Shafer, Alpha T. N'Diaye, David Johnson, Elke Arenholz, Bharat Jalan, Nigel D. Browning, and Yuri Suzuki. Magnetism and transport in transparent high-mobility $basno_3$ films doped with la, pr, nd, and gd. *Phys. Rev. Materials*, 3:124402, Dec 2019.

[16] J.T Rijssenbeek, R. Jin, Yu. Zadorozhny, Y. Liu, B. Batlogg, and R.J. Cava. Electrical and magnetic properties of the two crystallographic forms of $baruo_3$. *Phys. Rev. B*, 59:4561–4564, 1999.

[17] Yongmao Cai, Zu-Fei Huang, Xing Meng, Xing Ming, Chunzhong Wang, and Gang Chen. Pressure-induced phase transformation and magnetism transition in $baruo_3$: a first principles study. *Phys. Rev. B*, 13:350–356, 2011.

[18] M.K. Lee, C.B. Eom, J. Lettieri, I.W. Scrymgeour, D.G. Schlom, W. Tian, X.Q. Pan, P.A. Ryan, and F Tsui. Epitaxial thin films of hexagonal BaRuO 3 on (001) SrTiO 3. *Applied Physics Letters*, 78, 2001.

[19] C.Q. Jin, J.S. Zhou, J.B. Goodenough, Q.Q. Liu, J.G. Zhao, L.X. Yang, Y. Yu, R.C. Yu, T. Katsura, A Shatskiy, and E. Ito. High-pressure synthesis of the cubic perovskite baruo3 and evolution of ferromagnetism in aruo3 (a = ca, sr, ba) ruthenates. *PNAS*, 105:7115–7119, 2008.

[20] J.S. Zhou, K. Matsubayashi, Y. Uwatoko, C.Q. Jin, J.G. Cheng, J.B. Goodenough, Q.Q. Liu, T. Katsura, A. Shatskiy, and E. Ito. Critical behavior of the ferromagnetic perovskite $baruo_3$. *PRL*, 101:077206–1–4, 2012.

[21] J.G. Cheng, J.S. Zhou, J.B. Goodenough, and C.Q. Jin. Critical behavior of ferromagnetic perovskite ruthenates. *Phys. Rev. B*, 85:184430–1–7, 2012.

[22] Yingying Zhang, Zhangzhang Cui, Liuyang Zhu, Zhibo Zhao, Huan Liu, Qingmei Wu, Jianlin Wang, Haoliang Huang, Zhengping Fu, and Yalin Lu. Negative effect of oxygen vacancies on ferromagnetism in ru-doped basno3 materials. *Appl. Phys. Lett.*, 117:052406–1–4, 2020.

[23] J.S. Dodge, E. Kulatov, L. Klein, C.H. Ahn, J.W. Reiner, L. Mieville, T.H. Geballe, M.R. Beasely, A. Kapitulnik, H. Ohta, Yu. Uspenskii, and S. Halilov. Temperature-dependent local exchange splitting in $srruo_3$. *Phys. Rev. B*, 60:6987–6990, 1999.

[24] J.G. Cheng, J.S. Zhou, and J.B. Goodenough. Lattice effects on ferromagnetism in perovskite ruthenates. *PNAS*, 110:13312–13315, 2013.

[25] L. Klein, J.S. Dodge, C.H. Ahn, J.W. Reiner, L. Mieville, T.H. Geballe, M.R. Beasely, and A. Kapitulnik. Temperature-dependent local exchange splitting in $srruo_3$. *J. Phys.:Condensed Matter*, 8:10111–10126, 1996.

[26] G Santi and T. Jarlborg. Calculation of the electronic structure and the magnetic properties of $srruo_3$ and $caruo_3$. *J Phys Condens Matter*, 85:9563–9584, 1997.

[27] I.I. Mazin and D. J. Singh. Electronic structure and magnetism in ru-based perovskites. *Phys. Rev. B*, 56:2556–2571, 1997.

[28] Shivendra Tripathi, Rakesh Rana, Sanjay Kumar, Parul Pandey, R.S. Singh, and D.S. Rana. Ferromagnetic $caruo_3$. *Scientific Reports*, 4, 2014.